

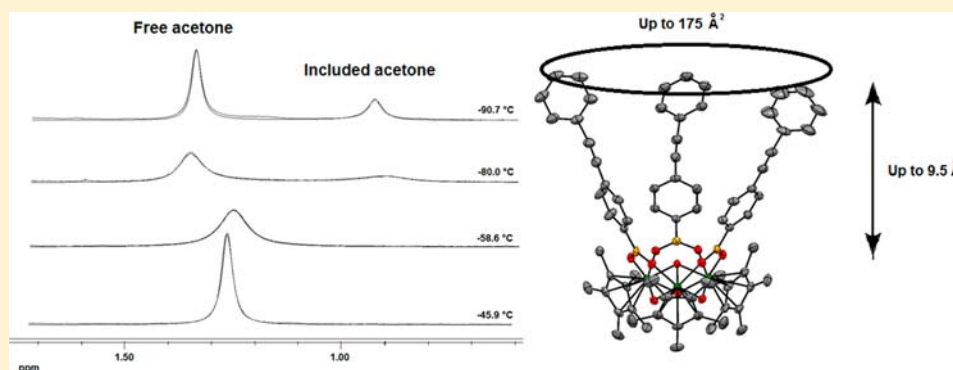
## On the Interaction of Acetone with Electrophilic Metallocavitands Having Extended Cavities

Christian N. Garon,<sup>†,‡</sup> Maxime Daigle,<sup>†,‡,§</sup> Isabelle Levesque,<sup>†,‡,§</sup> Philippe Dufour,<sup>†,§</sup> Hassan Iden,<sup>†,‡,§</sup> Christian Tessier,<sup>†</sup> Thierry Maris,<sup>||</sup> Jean-François Morin,<sup>†,§</sup> and Frédéric-Georges Fontaine<sup>\*,†,||</sup>

<sup>†</sup>Département de Chimie, <sup>‡</sup>Centre de Recherche sur la Propriété des Interfaces et de la Catalyse (CERPIC), and <sup>§</sup>Centre de Recherche sur les Matériaux Avancés (CERMA), Université Laval, 1045 Avenue de la Médecine, Québec, Québec, Canada, G1 V 0A6

<sup>||</sup>Département de Chimie, Université de Montréal, C.P. 6128 Succursale Centre-ville, Montréal, Québec, Canada, H3C 3J7

### S Supporting Information



**ABSTRACT:** We report the synthesis and characterization of tantalum–boronate trimetallic clusters of general formula  $\{[\text{Cp}^*\text{Ta}]_3(\mu^2\text{-RB}(\text{O})_2)_3(\mu^2\text{-OH})(\mu^2\text{-O})_2(\mu^3\text{-OH})\}$  ( $\text{R} = 4\text{-}(\text{C}_6\text{H}_5)(\text{C}_6\text{H}_4)$  ( $\text{Ta}_3\text{-4Ph}$ ),  $4\text{-}(\text{C}_6\text{H}_5\text{O})(\text{C}_6\text{H}_4)$  ( $\text{Ta}_3\text{-4OPh}$ ),  $4\text{-}(\text{C}_7\text{H}_7\text{O})(\text{C}_6\text{H}_4)$  ( $\text{Ta}_3\text{-4OBn}$ ),  $4\text{-}(\text{C}_8\text{H}_5)(\text{C}_6\text{H}_4)$  ( $\text{Ta}_3\text{-4PhEt}$ ), and  $4\text{-}(\text{C}_{12}\text{H}_7)(\text{C}_6\text{H}_4)$  ( $\text{Ta}_3\text{-4Napht}$ )). All complexes have been characterized by NMR spectroscopy and X-ray diffraction. The trimetallic species feature a large Lewis acid type cavity allowing for substrate binding in both the solid and the liquid state using a unique electrostatic interaction and a hydrogen bond.  $\Delta H^\circ$  and  $\Delta S^\circ$  values for association of acetone with the complexes vary between  $-2.0$  and  $-4.1$   $\text{kcal}\cdot\text{mol}^{-1}$  and  $-3$  and  $2$   $\text{cal}\cdot\text{mol}^{-1}\cdot\text{K}^{-1}$ , respectively, showing weaker binding than smaller cavities of the same type. The barrier for acetone exchange at equilibrium is similar for all complexes, and  $\Delta H^\ddagger$  values vary between  $8.2$  and  $11.4$   $\text{kcal}\cdot\text{mol}^{-1}$ .

## INTRODUCTION

Cavitands are a subcategory of supramolecular assemblies which possess a cavity able to host guest molecules. Much work underlining the importance of cavitands in supramolecular chemistry has been reported in the recent literature.<sup>1</sup> Indeed, molecules such as calixarenes,<sup>2</sup> cucurbiturils,<sup>3</sup> and cyclodextrins,<sup>4</sup> among others, can host smaller molecules within their structure and act as catalytic nanoreactors,<sup>5</sup> drug delivery agents,<sup>6</sup> or molecular detectors.<sup>7</sup> While these molecules exhibit remarkable versatility toward incorporation of a multitude of desired functional moieties within their structure, such sought-after functionalization can be synthetically very challenging and often requires multistep syntheses that hurt overall yields. The presence of one or many metal ions in the cavitand framework can yield interesting new properties, notably as shape-selective catalysts.<sup>8</sup> There are two pathways that can be devised to synthesize metallocavitands: either by introduction of Lewis basic buttresses on the cavitand to coordinate metal salts<sup>9</sup> or by addition of ligands with no specific hosting capability that will generate a metallocavitand upon coordination.<sup>10</sup> Of course, the

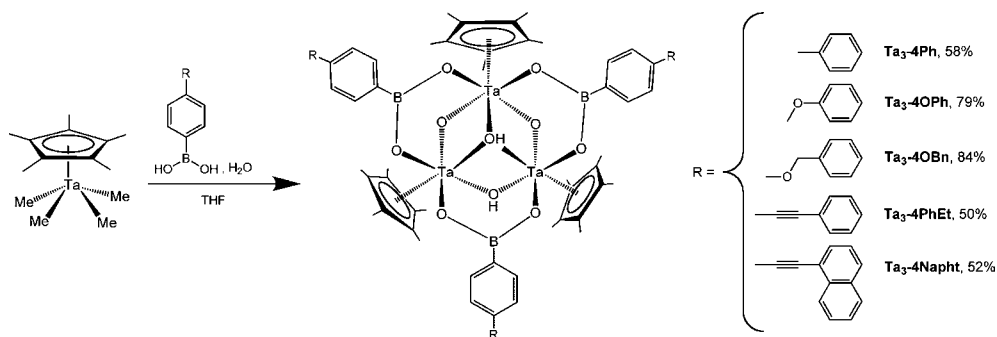
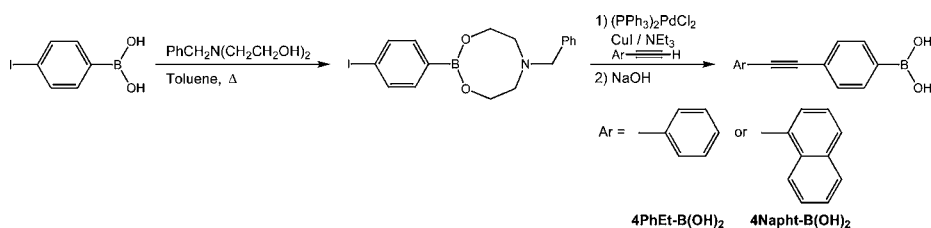
latter way has the major advantage of generating complex assemblies and ordered cavitands with little synthetic effort.

Although the coordination chemistry of carboxylate ligands has garnered much interest, notably in the synthesis of metal–organic frameworks,<sup>11</sup> relatively little work has been reported regarding its boron analogue, the boronate moiety. A handful of alkyl- and arylboronate complexes have been reported in the literature,<sup>12</sup> the majority with late transition metals in works related to Suzuki–Miyaura coupling reactions. This relative scarcity in the literature has to do with the weak B–C bond, which is susceptible to oxidative coupling. This issue can be addressed by coordination to oxophilic and high oxidation state early transition metals, which tend to form strong M–O bonds that stabilize ligand coordination.

We recently reported the preparation of a new class of tantalum–arylboration clusters exhibiting a cavity.<sup>13</sup> These metallocavitands can be generated in good yields through a one-step reaction of  $\text{Cp}^*\text{TaMe}_4$  with an arylboronic acid.

Received: July 19, 2012

Published: September 17, 2012

Scheme 1. Synthesis of Metallocavitands  $\text{Ta}_3\text{-4Ph}$ ,  $\text{Ta}_3\text{-4OPh}$ ,  $\text{Ta}_3\text{-4OBn}$ ,  $\text{Ta}_3\text{-4PhEt}$ , and  $\text{Ta}_3\text{-4Napht}$ Scheme 2. Synthesis of Boronic Acids  $4\text{PhEt-B(OH)}_2$  and  $4\text{Napht-B(OH)}_2$ 

Although the boron loses some of its Lewis acid character by donation from the oxygen atom in the metal oxide cluster, the presence of an electrophilic element such as boron in conjunction with the electropositive tantalum gives the cavity an overall electrophilic character, which has been demonstrated by the strong interaction with Lewis bases such as ketones and furans for those clusters, as previously observed in some aluminum cavitands.<sup>14</sup> We established the generality of the procedure and looked at the steric and electronic factors affecting the shape and size of the metallocavitand's cavity. Nevertheless, the overall volume of the cavities generated was quite limited. We report herein our efforts toward increasing the size of the cavity in our metallocavitands while maintaining the shape of the upper rim as undistorted as possible and our study in their hosting ability. In order to do so, several derivatives of phenylboronic acid functionalized in the para position were used, most featuring a delocalized  $\pi$  system.

## RESULTS AND DISCUSSION

**Synthesis and X-ray Diffraction Studies.** Following the established procedure,<sup>15</sup> complexes  $\{[\text{Cp}^*\text{Ta}]_3(\mu^2\text{-4-(C}_6\text{H}_5\text{)-(C}_6\text{H}_4\text{)B(O)}_2)_3(\mu^2\text{-O)}_2(\mu^2\text{-OH})(\mu^3\text{-OH})\}$  ( $\text{Ta}_3\text{-4Ph}$ ),  $\{[\text{Cp}^*\text{Ta}]_3(\mu^2\text{-4-(C}_6\text{H}_5\text{O)(C}_6\text{H}_4\text{)B(O)}_2)_3(\mu^2\text{-O)}_2(\mu^2\text{-OH})(\mu^3\text{-OH})\}$  ( $\text{Ta}_3\text{-4OPh}$ ),  $\{[\text{Cp}^*\text{Ta}]_3(\mu^2\text{-4-(C}_7\text{H}_7\text{O)(C}_6\text{H}_4\text{)B(O)}_2)_3(\mu^2\text{-O)}_2(\mu^2\text{-OH})(\mu^3\text{-OH})\}$  ( $\text{Ta}_3\text{-4OBn}$ ),  $\{[\text{Cp}^*\text{Ta}]_3(\mu^2\text{-4-(C}_6\text{H}_5\text{)-C}\equiv\text{C-(C}_6\text{H}_4\text{)B(O)}_2)_3(\mu^2\text{-O)}_2(\mu^2\text{-OH})(\mu^3\text{-OH})\}$  ( $\text{Ta}_3\text{-4PhEt}$ ), and  $\{[\text{Cp}^*\text{Ta}]_3(\mu^2\text{-4-(C}_{10}\text{H}_7\text{)-C}\equiv\text{C-(C}_6\text{H}_4\text{)B(O)}_2)_3(\mu^2\text{-O)}_2(\mu^2\text{-OH})(\mu^3\text{-OH})\}$  ( $\text{Ta}_3\text{-4Napht}$ ) were synthesized in moderate to good isolated yields as can be seen in Scheme 1. Whereas the boronic acids  $\text{C}_6\text{H}_5\text{-C}_6\text{H}_4\text{-B(OH)}_2$ ,  $\text{C}_6\text{H}_5\text{O-C}_6\text{H}_4\text{-B(OH)}_2$ , and  $\text{C}_7\text{H}_7\text{O-C}_6\text{H}_4\text{-B(OH)}_2$  were purchased and used as received,  $\text{C}_6\text{H}_5\text{-C}\equiv\text{C-C}_6\text{H}_4\text{-B(OH)}_2$  ( $4\text{PhEt-B(OH)}_2$ ) and  $\text{C}_{10}\text{H}_7\text{-C}\equiv\text{C-C}_6\text{H}_4\text{-B(OH)}_2$  ( $4\text{Napht-B(OH)}_2$ ) were synthesized using a Sonogashira reaction between the ester derived from protection of 4-iodophenylboronic acid with 1-benzyl-diethanolamine and the corresponding ethynyl reagent (Scheme 2 and Experimental Section for details). Solid state structures for all tantalum complexes could be solved from single crystals obtained

through slow evaporation of concentrated acetone or toluene solutions and can be seen in Figures 1–5. The representations with the included solvents can be found in the ESI.

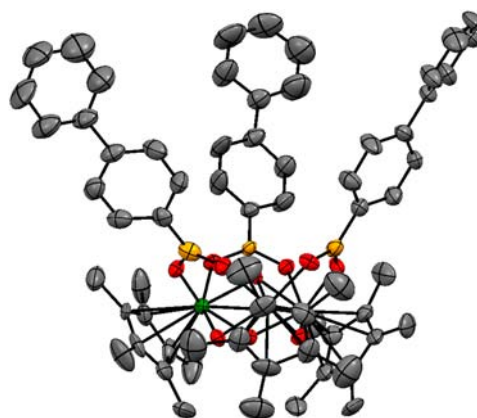
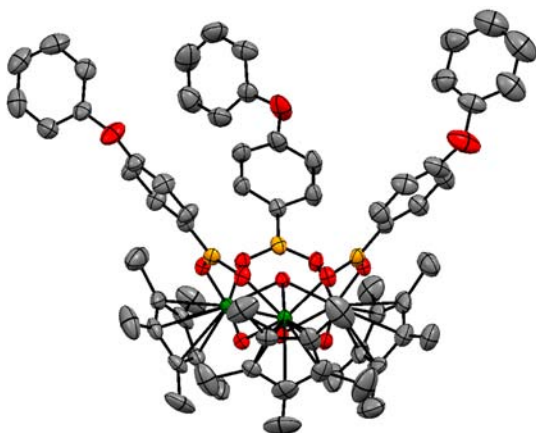


Figure 1. Thermal atomic displacement parameters diagram (50% probability) of  $\text{Ta}_3\text{-4Ph}$ . Hydrogen atoms and solvent molecules have been omitted for clarity: gray, carbon; red, oxygen; orange, boron; green, tantalum.

All compounds form the expected  $\text{Ta}_3\text{-O}_{10}$  inorganic core, the tantalum centers being in a pseudo-octahedral environment with the  $\text{Cp}^*$  ligands trans to the  $\mu^3\text{-OH}$  and the bridging boronates cis to the  $\mu^2\text{-oxygens}$ . The longer Ta1–Ta3 bond distances in  $\text{Ta}_3\text{-4Ph}$ ,  $\text{Ta}_3\text{-4OPh}$ ,  $\text{Ta}_3\text{-4PhEt}$ , and  $\text{Ta}_3\text{-4Napht}$  compared to the Ta1–Ta2 and Ta2–Ta3 distances suggest that these complexes possess a  $\text{C}_2$  symmetry created by the OH groups on O9 and O10 forming a mirror plane passing through one of the tantalum centers.  $\text{Ta}_3\text{-4OBn}$  exhibit the higher  $\text{C}_3$  symmetry one can expect from such trimetallic species in a rhombohedral space group. A table of all relevant distances can be seen in Table 1 as well as the numbering scheme employed throughout this report in Figure 6.

It is important to note that the apparent  $\text{C}_3$  symmetry displayed by  $\text{Ta}_3\text{-4OBn}$  is only observed in the solid state.



**Figure 2.** Thermal atomic displacement parameters diagram (50% probability) of  $\text{Ta}_3\text{-4OPh}$ . Hydrogen atoms and solvent molecules have been omitted for clarity: gray, carbon; red, oxygen; orange, boron; green, tantalum.

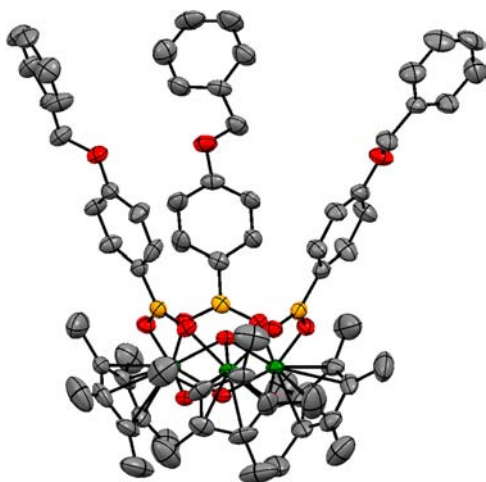


**Figure 3.** Thermal atomic displacement parameters diagram (50% probability) of  $\text{Ta}_3\text{-4OBn}$ . Hydrogen atoms and solvent molecules have been omitted for clarity: gray, carbon; red, oxygen; orange, boron; green, tantalum.

Indeed, inspection of the  $^1\text{H}$  NMR spectra of all complexes reveals two nonequivalent environments for the  $\text{Cp}^*$  ligands, with integration ratios of 2:1 consistent with  $\text{C}_2$  symmetry. The higher  $\text{C}_3$  symmetry therefore arises from the packing effect of the molecules in the crystal. With the exception of  $\text{Ta}_3\text{-4Napht}$ , all complexes crystallize with an acetone molecule trapped within the cavity and having weak van der Waals contacts with one of the boron centers ( $d_{\text{B-O}90}$  of 2.993 Å for  $\text{Ta}_3\text{-4Ph}$ , 2.995 Å for  $\text{Ta}_3\text{-4OPh}$ , 3.136 Å for  $\text{Ta}_3\text{-4OBn}$ , and 2.966 Å for  $\text{Ta}_3\text{-4PhEt}$ ) and significant hydrogen bonding with the  $\mu^3\text{-OH}$  ( $d_{\text{O}10\text{-O}90}$  of 2.640 Å for  $\text{Ta}_3\text{-4Ph}$ , 2.710 Å for  $\text{Ta}_3\text{-4OPh}$ , 2.668 Å for  $\text{Ta}_3\text{-4OBn}$ , and 2.621 Å for  $\text{Ta}_3\text{-4PhEt}$ ). Interestingly, two opposing orientations could be found for the acetone molecule within  $\text{Ta}_3\text{-4OPh}$ . The second orientation has the carbonyl oxygen almost equidistant from two of the boron centers and pointing away from the third. These two possible opposite orientations could arise from the increased width of the cavity of  $\text{Ta}_3\text{-4OPh}$  compared to the other three complexes. Indeed, the distances between the para carbons in the aryl boronate ligands ( $4\text{-R-C}_6\text{H}_4\text{BO}_2^{2-}$ ) are found to be averaging 10.063 Å in  $\text{Ta}_3\text{-4OPh}$ , whereas average

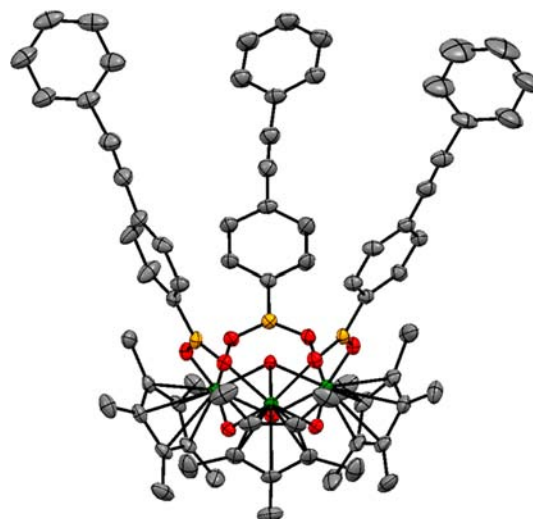


**Figure 4.** Thermal atomic displacement parameters diagram (50% probability) of  $\text{Ta}_3\text{-4PhEt}$ . Hydrogen atoms and solvent molecules have been omitted for clarity: gray, carbon; red, oxygen; orange, boron; green, tantalum.

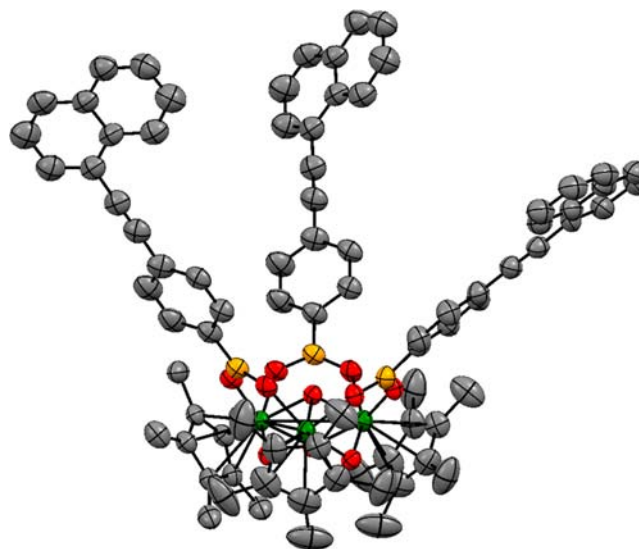


**Figure 5.** Thermal atomic displacement parameters diagram (50% probability) of  $\text{Ta}_3\text{-4Napht}$ . Hydrogen atoms and solvent molecules have been omitted for clarity: gray, carbon; red, oxygen; orange, boron; green, tantalum.

**Table 1. Distances of Interest in Structurally Characterized  $\text{Ta}_3$  Complexes<sup>a</sup>**

complex	$d_{\text{Ta}1\text{-Ta}2}$ (Å)	$d_{\text{Ta}2\text{-Ta}3}$ (Å)	$d_{\text{Ta}1\text{-Ta}3}$ (Å)	$d_{\text{Ta}1\text{-O}9}$ (Å)	$d_{\text{Ta}3\text{-O}9}$ (Å)	$d_{\text{C}90\text{-O}90}$ (Å)
$\text{Ta}_3\text{-4Ph}$	3.305	3.274	3.537	2.148	2.175	1.179
$\text{Ta}_3\text{-4OPh}$	3.322	3.295	3.477	2.116	2.131	1.198
$\text{Ta}_3\text{-4OBn}$	3.364	3.364	3.364	2.038	2.015	1.208
$\text{Ta}_3\text{-4PhEt}$	3.337	3.341	3.407	2.062	2.063	1.176
$\text{Ta}_3\text{-4Napht}$	3.300	3.300	3.499	2.136	2.136	

<sup>a</sup>Distances listed without ESDs and limited to 4 significant figures. Full values in the Supporting Information.

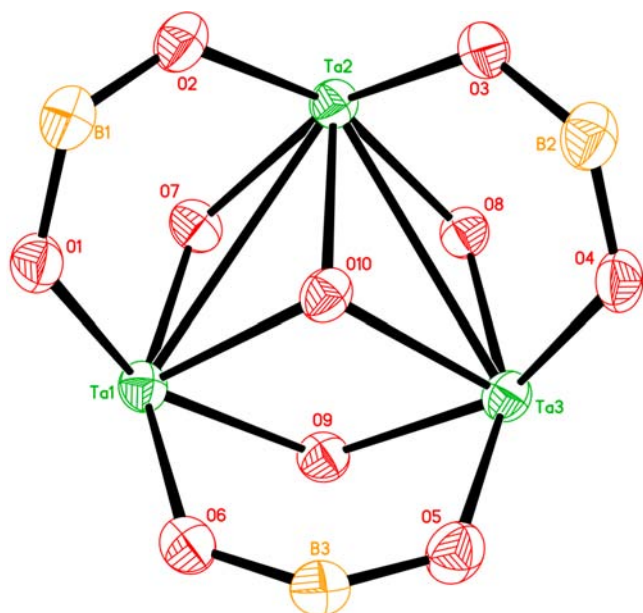


Figure 6. Labeling scheme for the inorganic core of  $Ta_3$  complexes.

values of 9.300, 8.157, and 9.065 Å were found for  $Ta_3$ -4Ph,  $Ta_3$ -4OBn, and  $Ta_3$ -4PhEt, respectively.

Complex  $Ta_3$ -4Ph also crystallizes with a highly disordered second acetone molecule outside of the cavity, providing invaluable support to the crystal lattice. Indeed, drying the crystals to try to get rid of the excess solvent molecules destroys them. The aromatic moieties of the boronate ligands in  $Ta_3$ -4Ph suffer a certain level of distortion from their expected planar configuration. Indeed, rotations averaging  $26^\circ$  out of the O–B–O plane can be observed for the first phenyl fragments, and further rotations along the C–C bond between the two aromatic rings average  $22^\circ$ . This results in one of the boronate ligands having its second aromatic ring almost perpendicular to the center of the cavity.

Complex  $Ta_3$ -4OPh was found to possess less rotational distortion in its boronate ligands, with ring rotations averaging only  $7^\circ$ . The aromatic phenoxide fragments are almost perpendicular to the first six-membered rings, and one of them points toward the center of the cavity, whereas the other two point away. Rotational disorder was also observed in the  $Cp^*$  moieties, and two positions could be determined. The least amount of distortions in the boronate ligands was observed in  $Ta_3$ -4OBn, which has rotations averaging  $2^\circ$ . The six-membered rings of the benzyloxy fragments all have their centers pointing toward the center of the cavity, and analysis of the packing system shows  $\pi$  interaction with the  $Cp^*$  ligands of adjacent molecules (Figure 7a).

In addition to two disordered toluene molecules in the crystal structure of  $Ta_3$ -4PhEt, including one toluene molecule located within the cavity of the metallocavitand with the included acetone, two of the three terminal phenyl groups exhibit significant rotational disorder, with the dihedral angles between the two aromatic rings being of  $21.0^\circ$ ,  $27.1^\circ$ , and  $87.3^\circ$ .

There are two possible orientations for the naphtyl group in one of the boronate ligands of  $Ta_3$ -4Napht caused by the presence of a mirror plane in the middle of the cavity. Indeed, two of the three boronate ligands are equivalent by symmetry, and the third possesses two different orientations that are the

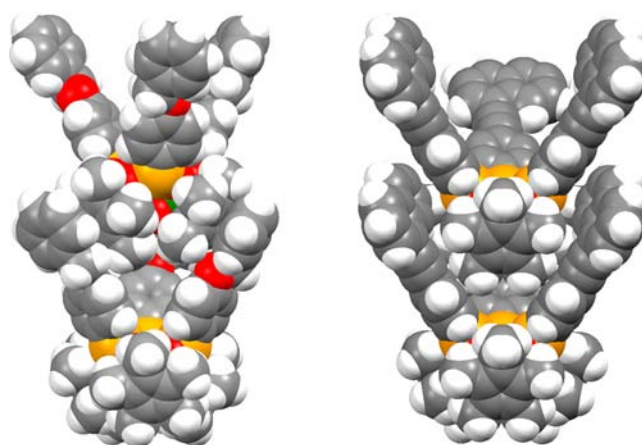


Figure 7. Space-filling representation of (a) two  $Ta_3$ -4OBn molecules (left) and (b) two  $Ta_3$ -4Napht molecules (right) showing the  $\pi$ -stacking between the outer phenyl moieties and the  $Cp^*$  ligands of the adjacent molecule: gray, carbon; white, hydrogen; red, oxygen; orange, boron; green, tantalum.

mirror representation of each other. This species is the only one that does not include acetone within the cavity but is still stabilized by the presence of two water molecules. As it was observed in the case of  $Ta_3$ -4OBn, the void of the cavittand is filled mainly by hosting the bottom of another cavittand (Figure 7b). However, whereas the interaction in  $Ta_3$ -4OBn is governed by  $\pi$ – $\pi$  interactions between the  $Cp^*$  of one cavittand and the terminal benzyl group of the  $C_6H_5$ – $CH_2O$ – $C_6H_4$ – $BO_2^{2-}$  ligand, the  $\pi$ – $\pi$  interactions in  $Ta_3$ -4Napht are governed by interaction of the phenyl group ( $C_{10}H_7$ – $C\equiv C$ – $C_6H_4$ – $BO_2^{2-}$ ) of one cavittand with the naphtyl group of another metallocavitand. As such, there is the presence of a pseudo- $S_3$  screw axis in  $Ta_3$ -4Napht compared with a pseudo- $S_6$  screw axis in  $Ta_3$ -4OBn (Figure 7).

Measurements were made to compare the height of the cavities in all metallocavitands synthesized in this study and compared to our previous work.<sup>13</sup> The height of the cavity is defined as the distance between the plane formed by the three boron centers and the plane formed by the three highest carbons on the upper rim (Figure 8). Table 2 gathers all data for the complexes.

Cavity heights of 6.982, 7.152, 8.919, 9.378, and 9.359 Å were found for complexes  $Ta_3$ -4Ph,  $Ta_3$ -4OPh,  $Ta_3$ -4OBn,

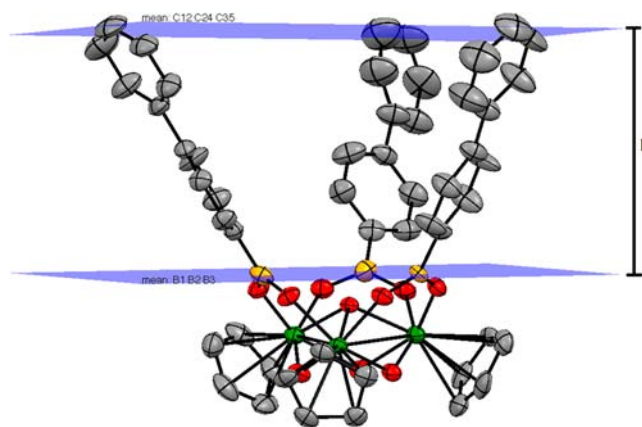
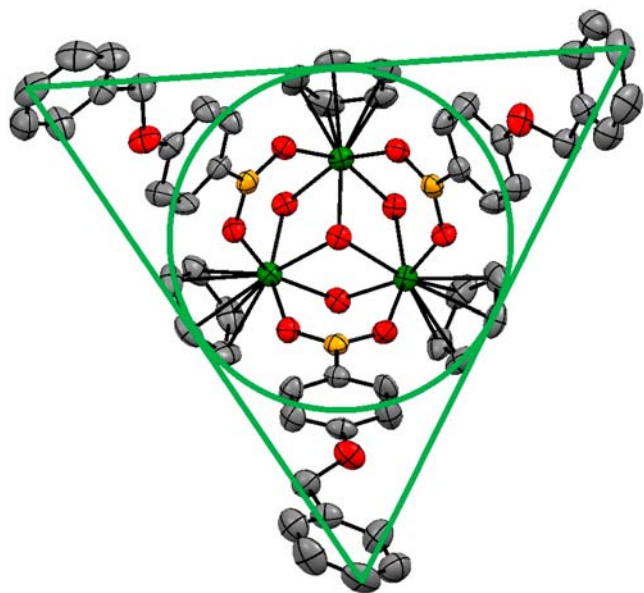


Figure 8. Distance ( $h$ ) between the two illustrated planes is the cavity height.

**Table 2. Cavity Heights and Upper Rim Area of the Structurally Characterized Ta<sub>3</sub> Complexes**

complex	cavity height (Å)	incircle area (Å <sup>2</sup> )
Ta <sub>3</sub> -Ph·THF	3.185	26
Ta <sub>3</sub> -Ph·Acetone	3.674	20
Ta <sub>3</sub> -3,5Me	3.676	20
Ta <sub>3</sub> -3,5CF <sub>3</sub>	3.897	17
Ta <sub>3</sub> -4Ph	6.982	46
Ta <sub>3</sub> -4OPh	7.215	47
Ta <sub>3</sub> -4OBn	8.919	55
Ta <sub>3</sub> -4PhEt	9.378	82
Ta <sub>3</sub> -4Napht	9.359	175

Ta<sub>3</sub>-4PhEt, and Ta<sub>3</sub>-4Napht, respectively. This clearly shows a net increase in the depth of the cavities compared to the complexes reported previously. We also compared the size of the upper rim of the metallocavitands by calculating the area of the incircle fitting inside the triangle formed by linking the highest carbon of each boronate ligand in the molecules (Figure 9). Data obtained is contained in Table 2.

**Figure 9.** Diagram showing the triangle formed by linking the highest carbons and the incircle used for the areas calculated.

These values can provide us with a general idea of the size of the cavity in our complexes. All complexes without substituents in the para position of the aryl fragment have similar values ranging from 17 (Ta<sub>3</sub>-3,5CF<sub>3</sub>) to 26 Å<sup>2</sup> (Ta<sub>3</sub>-Ph·THF).<sup>13</sup> Interestingly, complex Ta<sub>3</sub>-Ph crystallized in acetone has a smaller upper rim area (20 Å<sup>2</sup>) than Ta<sub>3</sub>-Ph crystallized in THF

(26 Å<sup>2</sup>). This clearly shows that while the metallocavitands have a fixed orientation, a certain level of flexibility while in solution is available and they can access wider or narrower conformations to best accommodate the guest molecules. The areas calculated for the expanded cavities show a net increase compared to the complexes unsubstituted in the para position. Both complexes Ta<sub>3</sub>-4Ph and Ta<sub>3</sub>-4OPh were found to have similar upper rim areas of 46 and 47 Å<sup>2</sup>, respectively. The similarity in these values despite the increased ligand size arises from folding of one of the boronate ligands toward the center of the cavity in Ta<sub>3</sub>-4OPh. Complex Ta<sub>3</sub>-4OBn exhibits an upper rim area with 55 Å<sup>2</sup>. As for complexes having acetynyl moieties, they exhibit significantly larger cavities, having incircle areas of 82 and 175 Å<sup>2</sup> for Ta<sub>3</sub>-4PhEt and Ta<sub>3</sub>-4Napht, respectively.

**Host–Guest Studies.** To probe the host–guest properties of our complexes, thermogravimetric analyses were done on the expanded cavity metallocavitands, and results are collected in Table 3. A dry ground sample of the complex is exposed to 3 drops of either acetone or THF and allowed to air dry, upon which it is placed into the TGA apparatus. The sample is left for 5 min at 30 °C to remove any excess solvent and then heated at 5 °C/min up to 200 °C. The tests done on the complexes exposed to acetone revealed that Ta<sub>3</sub>-4Ph, Ta<sub>3</sub>-4OBn, Ta<sub>3</sub>-4PhEt, and Ta<sub>3</sub>-4Napht all lose 1 equiv of acetone upon heating. When exposed to THF, Ta<sub>3</sub>-4Ph and Ta<sub>3</sub>-4OBn both lost 1 equiv while Ta<sub>3</sub>-4PhEt and Ta<sub>3</sub>-4Napht lost 2 equiv. These differences most likely have to do with size rather than specific differences in the interaction of the complexes, as they all feature a very wide open cavity. The temperatures at which acetone exited these metallocavitands optimally was similar and in the range of 104–115 °C for Ta<sub>3</sub>-4Ph, Ta<sub>3</sub>-4PhEt, and Ta<sub>3</sub>-4Napht. Ta<sub>3</sub>-4OBn gave a higher result with 131 °C. Interestingly, the results obtained from the experiments with THF all gave lower temperatures than for the tests with acetone, and the values observed are smaller than the majority of the smaller metallocavitands. Ta<sub>3</sub>-4Napht was even found to only have weak interaction with THF in the solid state, as evidenced by the 59 °C temperature observed, which is below the boiling point of THF. The general lower values observed with these complexes could be caused by the possibility for the substituents on the aryl group of the phenylboronate to undergo rotation around the C–C bond. Indeed, such interaction would weaken the interaction of the acetone with the cavity and favor its dissociation. Another explanation behind these values could be the thermal weakness of the expanded metallocavitands, which degraded at lower temperatures than for the smaller cavity complexes. Indeed, all complexes started to degrade soon after the guest molecules were gone, and Ta<sub>3</sub>-4OPh was even found to start decomposing at such low temperatures that the mass loss

**Table 3. TGA Studies of Ta<sub>3</sub> Complexes Exposed to Acetone or THF**

complex	acetone			THF		
	observed mass loss (%)	temp. (°C)	no. of solvent molecules lost	observed mass loss (%)	temperature (°C)	no. of solvent molecules lost
Ta <sub>3</sub> -4Ph	4.0	109	1	3.9	97	1
Ta <sub>3</sub> -4OPh						
Ta <sub>3</sub> -4OBn	2.6	131	1	3.3	89	1
Ta <sub>3</sub> -4PhEt	3.0	104	1	6.3	100	2
Ta <sub>3</sub> -4Napht	4.1	115	1	8.3	59	2

**Table 4.**  $^1\text{H}$  chemical shift of Bound and Free Acetone of  $\text{Ta}_3$  Complexes in Toluene- $d_8$  at Different Temperatures, Enthalpy ( $\Delta H^\circ$ ) and Entropy ( $\Delta S^\circ$ ) Associated with the Binding of Acetone within the Metallocavitands, and Activation Parameters ( $\Delta H^\ddagger$  and  $\Delta S^\ddagger$ ) of the Exchange between Free and Bound Acetone (see Figure 10)

complex	$\delta$ (ppm)		$\Delta H^\circ$ (kcal·mol $^{-1}$ )	$\Delta S^\circ$ (eu)	$\Delta H^\ddagger$ (kcal·mol $^{-1}$ )	$\Delta S^\ddagger$ (eu)
	22 °C	−80 °C				
free acetone	1.57	1.38				
$\text{Ta}_3$ -4Ph	1.44	0.81	$-3.4 \pm 0.6$	$-3 \pm 3$	$8.2 \pm 0.6$	$-6 \pm 3$
$\text{Ta}_3$ -4OPh	1.46	0.84	$-4.1 \pm 1.0$	$-6 \pm 3$	$11.4 \pm 0.8$	$9 \pm 4$
$\text{Ta}_3$ -4OBn	1.46	0.98	$-3.0 \pm 0.6$	$-4 \pm 2$	$8.5 \pm 0.9$	$-4 \pm 4$
$\text{Ta}_3$ -4PhEt	1.44	0.59	$-2.0 \pm 0.4$	$2 \pm 1$	$10.3 \pm 1.4$	$0 \pm 6$
$\text{Ta}_3$ -4Napht	1.44	0.71				

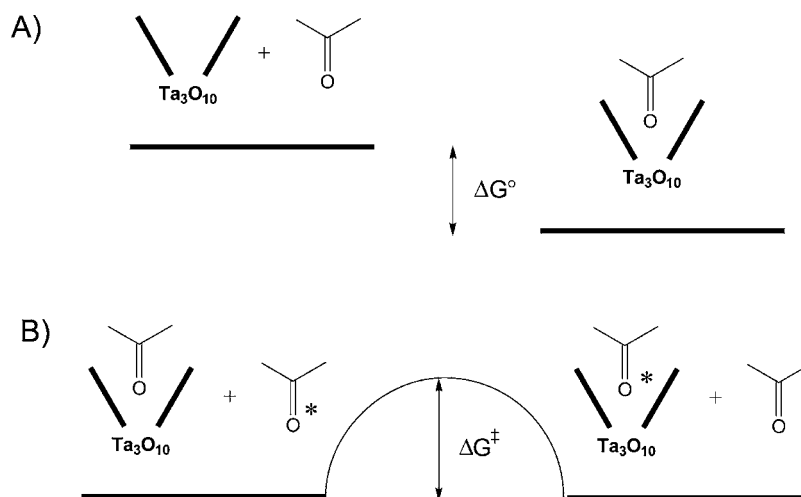


**Figure 10.** Representation of the thermodynamic (A) and kinetic (B) phenomenon in play in the  $^1\text{H}$  VT-NMR study of studied metallocavitands.

attributed to the exodus of the Lewis bases was indistinguishable from the mass loss due to decomposition.

In these systems, VT  $^1\text{H}$  NMR proved to be an excellent tool in order to determine the bonding interactions between acetone, acting as a guest, and the metallocavitand. It is possible to observe at 22 °C a significant shift of the included acetone in a toluene- $d_8$  solution containing one of the metallocavitands compared to that of acetone in a pure solution of toluene- $d_8$ . The chemical shift of 1 equiv of acetone is not greatly affected by the nature of the complex in solution varying in all cases from 1.44 to 1.46 ppm. The later resonances are significantly downfield from the acetone in the presence of species  $\{[\text{Cp}^*\text{Ta}]_3(\mu^2\text{-}(\text{C}_6\text{H}_5)\text{B}(\text{O})_2)_3(\mu^2\text{-O})_2(\mu^2\text{-OH})(\mu^3\text{-OH})\}$  ( $\text{Ta}_3\text{-Ph}$ ), which comes out at 1.34 ppm at room temperature, suggesting that the extended metallocavitands have weaker interaction with the weak Lewis base. Cooling down the temperature to  $-80$  °C allows the observation of two resonances for the acetone, one for the included species and another for free acetone. As shown in Table 4, the complexes exhibiting the most shielded resonances for the included acetone molecules are those with the extended conjugated  $\pi$  system, namely, species  $\text{Ta}_3$ -4PhEt and  $\text{Ta}_3$ -4Napht, where the chemical shift of the included acetone is observed at 0.59 and 0.71 ppm, respectively. Species  $\text{Ta}_3$ -4Ph and  $\text{Ta}_3$ -4OPh have the included acetone coming out at 0.81 and 0.84 ppm, respectively, whereas the species with the most flexibility,  $\text{Ta}_3$ -4OBn, exhibits the resonance at the lowest field at 0.98 ppm. These results suggest that the shielding of the methyl groups from the acetone molecule are not a consequence of the activation of the carbonyl group upon complexation with the

metallocavitand but rather from the anisotropy shielding of the aromatic signals of the boronate ligands that is more important in the conjugated  $\pi$  systems of  $\text{Ta}_3$ -4PhEt and  $\text{Ta}_3$ -4Napht.

Although determination of the association constants at very low temperature proved to be difficult because of the low solubility of some of the complexes, it was possible to determine these values at higher temperature using the shift of the acetone molecule at various temperatures (see Experimental Section for more details). Using the Van't Hoff equation, determination of the thermodynamic parameters  $\Delta H^\circ$  and  $\Delta S^\circ$  (Figure 10 A) was also possible for species  $\text{Ta}_3$ -4Ph,  $\text{Ta}_3$ -4OPh,  $\text{Ta}_3$ -4OBn, and  $\text{Ta}_3$ -4PhEt. A slight deviation from linearity arises at lower temperature, which can be attributed to the lower solubility of the complexes, but removal of these data points did not give significant modification of the thermodynamic parameters and were therefore kept in (see Supporting Information). The results confined in Table 4 show that the  $\Delta H^\circ$  values only slightly differ from one complex to another, varying from  $-2.0$  to  $-4.1$  kcal·mol $^{-1}$ , while  $\Delta S^\circ$  values are all very close to 0 cal·mol $^{-1}$ ·K $^{-1}$ . It should be kept in mind that two main factors are included in these thermodynamic parameters: (1) association of the acetone with the metallocavitand and (2) dissociation of the acetone–acetone interactions, which are known to be around 2–4 kcal·mol $^{-1}$  in organic solvents.<sup>15</sup> Therefore, the enthalpy related to association of the acetone with the cavitannds is between  $-4$  and  $-8$  kcal·mol $^{-1}$ . This relatively weak interaction is also supported by the entropy that is close 0 cal·mol $^{-1}$ ·K $^{-1}$ . Indeed, there is still significant freedom of movement for the included solvent that is on the same order to what is observed for

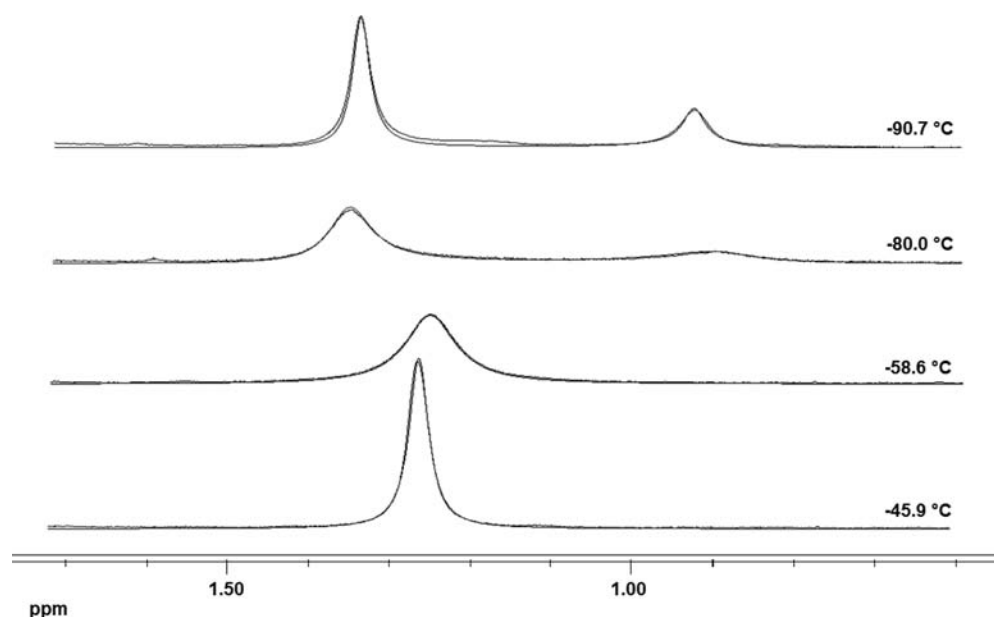


**Figure 11.** Low-temperature  $^1\text{H}$  NMR spectra of the acetone region for species  $\text{Ta}_3\text{-4OBn}$  with 2 equiv of acetone with overlay of the WINDNMR simulation.

acetone in organic solvents. Binding energies are significantly lower than in the smaller metallocavitands, such as  $\text{Ta}_3\text{-Ph}$ , where the binding energies were found using DFT to vary between  $-13$  and  $-16$   $\text{kcal}\cdot\text{mol}^{-1}$  depending on the nature of the substituents on the aryl group.<sup>13</sup> Therefore, it seems that association of acetone is possible in the larger cavitands but that having larger substituents on the boronate moiety greatly affects the interaction of the acetone with the core of the complexes. It is likely that the freedom of movement around the  $\text{sp}^2$  C–C bonds disfavors positioning of the Lewis base within the cavity.

It was also possible to do  $^1\text{H}$  NMR simulation of the two acetone resonances at low temperature in order to determine the exchange rates between the bound acetone and the free acetone at equilibrium at a given temperature (Figure 10 B). As can be observed in Figure 11, the models are quite representative of the experimental data and Eyring plots allow determination of the activation parameters that are summarized in Table 4. Once again, there are only slight differences in the  $\Delta H^\ddagger$  and  $\Delta S^\ddagger$  values obtained from one complex to another, ranging from 8.2 to 11.4  $\text{kcal}\cdot\text{mol}^{-1}$  and  $-6$  to 9 eu, respectively. The significantly larger  $\Delta H^\ddagger$  values compared to the  $\Delta H^\circ$  values support the hypothesis that two main entropic contributions are needed in order for the exchange to take place, which are dissociation of the metallocavitand–acetone interaction and that of the acetone–acetone interaction. Indeed,  $\Delta H^\ddagger$  values should be the summation of the energy to break acetone–metallocavitand interactions and acetone–acetone interactions. Therefore, according to the discussion in the above paragraph,  $\Delta H^\ddagger$  values should be between 6 and 12  $\text{kcal}\cdot\text{mol}^{-1}$ , which is in the range of the experimental data.

## CONCLUSION

The tritantalum clusters synthesized and structurally characterized in this report all possess a pseudo- $\text{C}_3$  symmetry that is broken in solution or in the solid state by the presence of two hydroxide groups in the  $\text{Ta}_3\text{O}_{10}$  inorganic core. It is possible to easily modify the nature of the cavity by modifying the nature of the boronic acid used in the synthesis of the cavitant,

increasing drastically the height of the cavitant from 3 to 4 Å in the simple metallocavitands up to 9 Å in the extended  $\pi$  systems. In the case of species  $\text{Ta}_3\text{-4OBn}$  and  $\text{Ta}_3\text{-4Napht}$ , there is stacking of the metallocavitand by incorporation of the end of one cavitant in the cavity of another one. Although these species possess the same ability to coordinate acetone molecules within their cavity, the binding energy was found to be significantly lower in the larger cavitands compared with the smaller ones. Indeed,  $\Delta H^\circ$  values were found to be around 2–3  $\text{kcal}\cdot\text{mol}^{-1}$ , which is about 10  $\text{kcal}\cdot\text{mol}^{-1}$  less than in the smallest cavities, which was confirmed using thermogravimetric analyses. Nevertheless, the possibility to modify the nature of the cavitant and thereby its overall volume can still show some advantages in hosting larger molecules that could have significant  $\pi$ – $\pi$  interactions, notably fullerenes. The possibility to further modulate the cavity lead us to believe that these extended cavities could play an important role in binding complex guests molecules. Such work is currently in progress.

## EXPERIMENTAL SECTION

**General Comments.** Syntheses of the tantalum clusters were conducted under an atmosphere of nitrogen using standard glovebox techniques. All subsequent manipulations and workup were done under normal atmosphere. Toluene was purified over Na/benzophenone, and other solvents were purified using a solvent purification system (VAC atmosphere). Benzene- $d_6$  and toluene- $d_8$  were purified by vacuum distillation from Na/K alloy. Elemental analyses were performed at the Laboratoire d'analyse élémentaire de l'Université de Montréal.  $\text{Cp}^*\text{TaMe}_4$  was prepared according to literature procedures.<sup>16</sup> Boronic acids  $\text{C}_6\text{H}_5\text{-C}_6\text{H}_4\text{-B(OH)}_2$ ,  $\text{C}_6\text{H}_5\text{O-C}_6\text{H}_4\text{-B(OH)}_2$ , and  $\text{C}_7\text{H}_7\text{O-C}_6\text{H}_4\text{-B(OH)}_2$  were purchased from Aldrich, Alfa Aesar, and Frontier Scientific and used as received. NMR spectra were recorded on a Varian Inova NMR AS400 spectrometer at 400.0 ( $^1\text{H}$ ) and 100.0 MHz ( $^{13}\text{C}$ ) or on a Bruker NMR AC-300 at 300 ( $^1\text{H}$ ) and 75.5 MHz ( $^{13}\text{C}$ ). Temperatures of the VT NMR experiments were measured using a thermocouple inside the probe which was calibrated with a capillary of methanol inside the sample.

**Synthesis of 1-Benzylidiethanolamine (1).** A 500 mL one-necked round bottomed flask equipped with a magnetic stir bar and a

reflux condenser was charged with diethanolamine (10.5 g, 100 mmol), anhydrous potassium carbonate (30 g, excess), benzyl bromide (17.2 g, 100 mmol), and dry acetone (250 mL). The reaction mixture was heated at reflux for 16 h with good stirring. After the reaction was completed, the reaction mixture was cooled, the potassium salt was filtered, and the reaction mixture was concentrated under reduced pressure. The residue was extracted with chloroform (3 × 100 mL) and washed with brine (2 × 200 mL). The organic layer was dried over MgSO<sub>4</sub>, filtered, and concentrated under reduced pressure to yield a colorless oil, which was further purified on a short plug of silica using EtOAc as eluent to yield the product as a colorless oil in quantitative yield. <sup>1</sup>H NMR (chloroform-*d*): δ 7.33–7.21 (m, 5H), 3.67 (s, 2H), 3.60–3.57 (d, *J* = 5.2 Hz, 4H), 2.69–2.66 (d, *J* = 5.2 Hz, 4H). <sup>13</sup>C{<sup>1</sup>H} NMR (chloroform-*d*): δ 138.6, 128.9, 128.4, 59.6, 59.2, 55.7. HRMS (EI) *m/z* 196.1331 [M + H; calcd for C<sub>11</sub>H<sub>18</sub>NO<sub>2</sub> 196.1332].

**Synthesis of 6-Benzyl-2-(4-iodophenyl)-1,3,6,2-dioxazaborocane (2).** A 100 mL one-necked round bottomed flask equipped with a magnetic stir bar and a Dean–Stark trap was charged with 4-iodophenylboronic acid (1.24 g, 5 mmol), **1** (0.97 g, 5 mmol) and dry toluene (250 mL). The reaction mixture was heated at reflux for 2.5 h in a 120 °C oil bath. The reaction was considered complete when evolution of water ceased. The solution was then concentrated under reduced pressure on a rotary evaporator to afford a white solid residue. This solid residue was dissolved in 100 mL of chloroform and washed with a saturated solution of sodium bicarbonate (2 × 100 mL). The layers were separated, and the organic product was dried over MgSO<sub>4</sub>, filtered, and concentrated under reduced pressure to yield the desired product as a white solid (1.93 g, 95%). Mp 170–172 °C. <sup>1</sup>H NMR (chloroform-*d*): δ 7.69–7.65 (m, 2H), 7.49–7.45 (m, 2H), 7.39–7.33 (m, 3H), 7.23–7.19 (m, 2H), 4.18 (t, *J* = 6.1 Hz, 4H), 3.37 (s, 2H), 3.32–3.14 (m, 2H), 2.90–2.76 (m, 2H). <sup>13</sup>C{<sup>1</sup>H} NMR (chloroform-*d*): δ 136.5, 135.5, 132.3, 131.0, 129.2, 128.9, 94.6, 63.0, 56.6. HRMS (EI) *m/z* 408.063 [M + H<sup>+</sup>; calcd for C<sub>17</sub>H<sub>20</sub>BINO<sub>2</sub>: 408.0629].

**Synthesis of C<sub>8</sub>H<sub>5</sub>–C<sub>6</sub>H<sub>4</sub>–B(OH)<sub>2</sub> (4PhEt-B(OH)<sub>2</sub>).** A 50 mL round bottomed flask equipped with a magnetic stir bar was charged with **2** (0.21 g, 0.52 mmol), CuI (0.003 g, 0.016 mmol), (Ph<sub>3</sub>P)<sub>2</sub>PdCl<sub>2</sub> (0.022 g, 0.03 mmol), and triethylamine (0.36 mL, 2.6 mmol) in degassed toluene (20 mL) and stirred at room temperature under argon for 20 min. 1-Ethynylbenzene (271 mg, 2.76 mmol) was added to the reaction mixture over 5 min and stirred at room temperature for an additional 2 h. A white precipitate was formed; the precipitate was filtered and washed with hexanes (30 mL). The precipitate was dissolved in 10 mL of dichloromethane followed by addition of 10 mL of 1 M HCl, the mixture was stirred for 30 min at room temperature, and the layers were separated. The aqueous layer was extracted with dichloromethane (2 × 10 mL). The organic layers were combined, dried over MgSO<sub>4</sub>, and concentrated to dryness. The solid residue was dissolved in dichloromethane (20 mL), and 1 M NaOH was added. The solution was stirred for 10 min at room temperature, the layers were separated, and the aqueous layer was acidified with 1 M HCl until pH ≈ 2 and extracted twice with dichloromethane (2 × 15 mL). The combined extracts were dried over MgSO<sub>4</sub> and concentrated to dryness to yield compound **4PhEt-B(OH)<sub>2</sub>** as an off-white solid (0.086 g, 75%). Mp 206–210 °C. <sup>1</sup>H NMR (chloroform-*d*): δ 8.16 (s, 2H), 7.80 (m, 2H), 7.55–7.52 (m, 2H), 7.49 (m, 2H), 7.40 (m, 3H). <sup>13</sup>C{<sup>1</sup>H} NMR (chloroform-*d*): δ 134.2, 131.3, 130.2, 128.8, 128.7, 123.6, 122.2, 90.0, 89.5. The C-B was not detected. HRMS (EI) *m/z* 222.083 [M<sup>+</sup>; calcd for C<sub>14</sub>H<sub>11</sub>BO<sub>2</sub> 222.085].

**Synthesis of C<sub>12</sub>H<sub>7</sub>–C<sub>6</sub>H<sub>4</sub>–B(OH)<sub>2</sub> (4Napht-B(OH)<sub>2</sub>).** Compound **4** was prepared following the same procedure described for synthesis of compound **3** with the following exceptions: 1-ethynylbenzene was substituted for 1-ethynyl naphthalene. The product was obtained as an off-white solid (0.13 g, 48%). Mp 255–258 °C. <sup>1</sup>H NMR (chloroform-*d*): δ 8.40–8.35 (m, 1H), 8.25 (s, 2H), 8.03–7.99 (m, 2H), 7.90–7.86 (m, 2H), 7.83 (m, 1H), 7.71–7.60 (m, 4H), 7.56 (m, 1H). <sup>13</sup>C{<sup>1</sup>H} NMR (chloroform-*d*): δ 134.4, 132.8, 132.4, 130.5, 130.4, 129.2, 128.5, 127.4, 126.8, 125.7, 125.5, 123.7, 119.7, 94.6, 88.0. The C-B was not detected. HRMS (EI) *m/z* 272.1006 [M<sup>+</sup>; calcd for C<sub>18</sub>H<sub>13</sub>BO<sub>2</sub> 272.1009].

**Synthesis of {[Cp\*Ta]<sub>3</sub>(μ<sup>2</sup>-4-(C<sub>6</sub>H<sub>5</sub>)(C<sub>6</sub>H<sub>4</sub>)B(O)<sub>2</sub>)<sub>3</sub>(μ<sup>2</sup>-O)<sub>2</sub>(μ<sup>2</sup>-OH)(μ<sup>3</sup>-OH)} (Ta<sub>3</sub>-4Ph).** A solution of water (4.8 μL, 0.266 mmol) and 4-(C<sub>6</sub>H<sub>5</sub>)C<sub>6</sub>H<sub>4</sub>B(OH)<sub>2</sub> (105 mg, 0.531 mmol) in THF (5 mL) was added to a solution of Cp\*TaMe<sub>4</sub> (100 mg, 0.266 mmol) in THF (5 mL) under nitrogen at –78 °C. The resulting yellow solution was stirred for 2 days at room temperature until it turned colorless. The solvent was then removed under reduced pressure. The resulting white precipitate was washed once with acetone (2 mL) in normal atmosphere. The white powder was dried for 1 h under vacuum, and colorless crystals were obtained from the acetone wash solution. Isolated yield: 0.083 mg, 58%. <sup>1</sup>H NMR (benzene-*d*<sub>6</sub>): δ 8.32 (br s, 4H), 8.11 (br d, <sup>3</sup>*J*<sub>H–H</sub> = 7.2 Hz, 2H), 7.62 (br d, <sup>3</sup>*J*<sub>H–H</sub> = 7.5 Hz, 4H), 7.53 (br d, <sup>3</sup>*J*<sub>H–H</sub> = 7.2 Hz, 4H), 7.43 (br d, <sup>3</sup>*J*<sub>H–H</sub> = 7.7 Hz, 2H), 7.34 (br s, 2H), 7.20 (m, 4H), 7.08 (m, 5H), 2.20 (ov s, 30 H), 2.13 (ov s, 15 H). μ<sup>2</sup>-OH and μ<sup>3</sup>-OH were not located. <sup>13</sup>C{<sup>1</sup>H} NMR (benzene-*d*<sub>6</sub>): δ 142.4, 142.3, 142.2, 136.6, 136.0, 133.5, 129.0, 128.6, 127.4, 127.2, 126.5, 126.4, 122.7, 122.2, 12.0, 11.6. HRMS (EI) *m/z* 1625.39282 [M + Na<sup>+</sup>; calcd for C<sub>66</sub>H<sub>77</sub>B<sub>3</sub>O<sub>10</sub>Ta<sub>3</sub>·Na 1625.3932].

**Synthesis of {[Cp\*Ta]<sub>3</sub>(μ<sup>2</sup>-4-(C<sub>6</sub>H<sub>5</sub>O)(C<sub>6</sub>H<sub>4</sub>)B(O)<sub>2</sub>)<sub>3</sub>(μ<sup>2</sup>-O)<sub>2</sub>(μ<sup>2</sup>-OH)(μ<sup>3</sup>-OH)} (Ta<sub>3</sub>-4OPh).** A solution of water (4.8 μL, 0.266 mmol) and 4-(C<sub>6</sub>H<sub>5</sub>O)C<sub>6</sub>H<sub>4</sub>B(OH)<sub>2</sub> (114 mg, 0.531 mmol) in THF (5 mL) was added to a solution of Cp\*TaMe<sub>4</sub> (100 mg, 0.266 mmol) in THF (5 mL) under nitrogen at –78 °C. The same procedure as Ta<sub>3</sub>-4Ph was followed. Isolated yield: 0.116 g, 79%. <sup>1</sup>H NMR (benzene-*d*<sub>6</sub>): δ 8.14 (br s, 4H), 7.99 (br d, <sup>3</sup>*J*<sub>H–H</sub> = 8.1 Hz, 2H), 7.08–6.80 (m, 21H), 2.15 (ov s, 30 H), 2.06 (ov s, 15 H). μ<sup>2</sup>-OH and μ<sup>3</sup>-OH were not located. <sup>13</sup>C{<sup>1</sup>H} NMR (benzene-*d*<sub>6</sub>): δ 159.1, 157.9, 137.7, 137.3, 134.7, 129.9, 123.3, 122.5, 119.5, 119.4, 118.0, 117.9, 11.9, 11.6. HRMS (EI) *m/z* 1673.37502 [M + Na<sup>+</sup>; calcd for C<sub>66</sub>H<sub>74</sub>B<sub>3</sub>O<sub>13</sub>Ta<sub>3</sub>·Na 1673.37407].

**Synthesis of {[Cp\*Ta]<sub>3</sub>(μ<sup>2</sup>-4-(C<sub>7</sub>H<sub>7</sub>O)(C<sub>6</sub>H<sub>4</sub>)B(O)<sub>2</sub>)<sub>3</sub>(μ<sup>2</sup>-O)<sub>2</sub>(μ<sup>2</sup>-OH)(μ<sup>3</sup>-OH)} (Ta<sub>3</sub>-4OBn).** A solution of water (4.8 μL, 0.266 mmol) and 4-(C<sub>6</sub>H<sub>5</sub>CH<sub>2</sub>O)C<sub>6</sub>H<sub>4</sub>B(OH)<sub>2</sub> (121 mg, 0.531 mmol) in THF (5 mL) was added to a solution of Cp\*TaMe<sub>4</sub> (100 mg, 0.266 mmol) in THF (5 mL) under nitrogen at –78 °C. The same procedure as Ta<sub>3</sub>-4Ph was followed. Isolated yield: 0.126 g, 84%. <sup>1</sup>H NMR (benzene-*d*<sub>6</sub>): δ 8.19 (br s, 4H), 8.07 (br d, <sup>3</sup>*J*<sub>H–H</sub> = 8.4 Hz, 1H), 7.25–7.18 (m, 6H), 7.12–6.99 (m, 15H), 6.91 (d, <sup>3</sup>*J*<sub>H–H</sub> = 8.6 Hz, 1H), 4.77 (s, 4H), 4.62 (s, 2H), 2.18 (ov s, 30 H), 2.10 (ov s, 15 H). <sup>13</sup>C{<sup>1</sup>H} NMR (benzene-*d*<sub>6</sub>): δ 160.8, 160.7, 138.2, 138.0, 137.7, 137.2, 131.7, 128.6, 127.6, 122.5, 122.1, 114.3, 114.1, 69.7, 69.5, 12.0, 11.7. HRMS (EI) *m/z* 1693.43939 [M + H<sup>+</sup>; calcd for C<sub>69</sub>H<sub>81</sub>B<sub>3</sub>O<sub>13</sub>Ta<sub>3</sub>·H 1693.43907].

**Synthesis of {[Cp\*Ta]<sub>3</sub>(μ<sup>2</sup>-4-(C<sub>8</sub>H<sub>5</sub>)(C<sub>6</sub>H<sub>4</sub>)B(O)<sub>2</sub>)<sub>3</sub>(μ<sup>2</sup>-O)<sub>2</sub>(μ<sup>2</sup>-OH)(μ<sup>3</sup>-OH)} (Ta<sub>3</sub>-4PhEt).** A solution of water (4.0 μL, 0.223 mmol) and **3** (99 mg, 0.446 mmol) in THF (5 mL) was added to a solution of Cp\*TaMe<sub>4</sub> (84 mg, 0.266 mmol) in THF (5 mL) under nitrogen at –78 °C. The same procedure as Ta<sub>3</sub>-4Ph was followed. Isolated yield: 0.061 g, 50%. <sup>1</sup>H NMR (benzene-*d*<sub>6</sub>): δ 8.17 (br s, 4H), 8.01 (br d, <sup>3</sup>*J*<sub>H–H</sub> = 7.1 Hz, 1H), 7.71 (br d, <sup>3</sup>*J*<sub>H–H</sub> = 8.1 Hz, 4H), 7.61 (br d, <sup>3</sup>*J*<sub>H–H</sub> = 7.8 Hz, 2H), 7.55–7.38 (m, 6H), 7.01–6.88 (m, 10H), 2.10 (ov s, 30 H), 2.03 (ov s, 15 H). <sup>13</sup>C{<sup>1</sup>H} NMR (benzene-*d*<sub>6</sub>): δ 139.9, 135.9, 135.4, 133.6, 132.0, 131.2, 131.0, 127.4, 124.8, 124.2, 122.8, 122.4, 91.1, 90.5, 11.9, 11.6. HRMS (EI) *m/z* 1697.38772 [M + Na<sup>+</sup>; calcd for C<sub>72</sub>H<sub>74</sub>B<sub>3</sub>O<sub>10</sub>Ta<sub>3</sub>·Na 1697.38932].

**Synthesis of {[Cp\*Ta]<sub>3</sub>(μ<sup>2</sup>-4-(C<sub>12</sub>H<sub>7</sub>)(C<sub>6</sub>H<sub>4</sub>)B(O)<sub>2</sub>)<sub>3</sub>(μ<sup>2</sup>-O)<sub>2</sub>(μ<sup>2</sup>-OH)(μ<sup>3</sup>-OH)} (Ta<sub>3</sub>-4Napht).** A solution of water (3.0 μL, 0.167 mmol) and **4** (92 mg, 0.335 mmol) in THF (5 mL) was added to a solution of Cp\*TaMe<sub>4</sub> (63 mg, 0.167 mmol) in THF (5 mL) under nitrogen at –78 °C. The same procedure as Ta<sub>3</sub>-4Ph was followed. Isolated yield: 0.053 mg, 52%. <sup>1</sup>H NMR (benzene-*d*<sub>6</sub>): δ 8.73 (br d, <sup>3</sup>*J*<sub>H–H</sub> = 7.5 Hz, 2H), 8.63 (br d, <sup>3</sup>*J*<sub>H–H</sub> = 7.5 Hz, 1H), 8.21 (br s, 4H), 8.09 (br d, <sup>3</sup>*J*<sub>H–H</sub> = 7.5 Hz, 2H), 7.76 (br d, <sup>3</sup>*J*<sub>H–H</sub> = 8.1 Hz, 4H), 7.67–7.63 (m, 3H), 7.55–7.45 (m, 6H), 7.40 (br d, <sup>3</sup>*J*<sub>H–H</sub> = 7.8 Hz, 1H), 7.37–7.33 (m, 3H), 7.28–7.19 (m, 4H), 7.04 (d, <sup>3</sup>*J*<sub>H–H</sub> = 8.3 Hz, 1H), 7.02 (br d, <sup>3</sup>*J*<sub>H–H</sub> = 8.3 Hz, 1H), 6.96–6.94 (m, 1H), 2.16 (ov s, 30 H), 2.07 (ov s, 15 H). <sup>13</sup>C{<sup>1</sup>H} NMR (benzene-*d*<sub>6</sub>): δ 135.8, 135.4, 134.0, 133.7, 133.5, 132.0, 131.3, 131.0, 130.7, 127.6, 127.1, 127.0, 126.8, 126.7, 126.6, 126.5, 125.5, 124.9, 122.8, 122.4, 121.8, 121.6,

Table 5. Crystallographic Data for the Reported Complexes

	Ta <sub>3</sub> -4Ph	Ta <sub>3</sub> -4OPh	Ta <sub>3</sub> -4OBn	Ta <sub>3</sub> -4PhEt	Ta <sub>3</sub> -4Napht
formula	2(C <sub>66</sub> H <sub>72</sub> B <sub>3</sub> O <sub>10</sub> Ta <sub>3</sub> ), 3(C <sub>3</sub> H <sub>6</sub> O)	C <sub>66</sub> H <sub>72</sub> B <sub>3</sub> O <sub>13</sub> Ta <sub>3</sub> , C <sub>3</sub> H <sub>6</sub> O	C <sub>69</sub> H <sub>78</sub> B <sub>3</sub> O <sub>13</sub> Ta <sub>3</sub> , C <sub>3</sub> H <sub>6</sub> O	2(C <sub>72</sub> H <sub>75</sub> B <sub>3</sub> O <sub>10</sub> Ta <sub>3</sub> ), C <sub>14</sub> H <sub>15</sub> , C <sub>7</sub> H <sub>8</sub> , 2(C <sub>3</sub> H <sub>6</sub> O)	C <sub>84</sub> H <sub>81</sub> B <sub>3</sub> O <sub>10</sub> Ta <sub>3</sub> , 2(C <sub>7</sub> H <sub>8</sub> ), 2(H <sub>2</sub> O)
fw	3375.27	1706.59	1748.67	3742.75	2046.07
cryst syst	monoclinic	triclinic	rhombohedral	monoclinic	orthorhombic
space group	P2/c	P-1	R3c	P2 <sub>1</sub> /n	Pbcm
a (Å)	24.189(4)	12.3989(12)	15.1087(5)	12.5477(4)	10.0015(12)
b (Å)	11.770(2)	12.5270(12)	15.1087(5)	31.1331(10)	32.004(4)
c (Å)	24.316(4)	22.486(2)	15.1087(5)	19.3082(6)	26.426(3)
α, β, γ (deg)	90, 101.937(3), 90	78.317(1), 76.609(1), 77.798(1)	94.35, 94.35, 94.35	90, 91.000(2), 90	90, 90, 90
V (Å <sup>3</sup> )	6774(2)	3277.3(5)	3417.5(2)	7541.6(4)	8458.5(17)
Z	2	2	2	2	4
D <sub>calcd</sub> (g·cm <sup>-3</sup> )	1.655	1.729	1.699	1.648	1.607
F <sub>000</sub>	3320	1676	1724	3710	4076
no. of unique/total reflins	13 316/68 889	10 989/36 857	4964/37 706	14 478/192 621	8322/163 099
R <sub>int</sub>	0.0723	0.0242	0.0509	0.049	0.083
goodness-of-fit on F <sup>2</sup>	1.385	1.278	1.124	1.043	1.043
final R indices [I > 2σ(I)]	R1 = 0.0513, wR2 = 0.1137	R1 = 0.0303, wR2 = 0.0742	R1 = 0.0265, wR2 = 0.0466	R1 = 0.0311, wR2 = 0.0798	R1 = 0.0584, wR2 = 0.1558

96.0, 88.7, 11.9, 11.6. HRMS (EI) *m/z* 1847.43372 [M + Na<sup>+</sup>; calcd for C<sub>84</sub>H<sub>80</sub>B<sub>3</sub>O<sub>10</sub>Ta<sub>3</sub>Na 1847.43627].

**Thermogravimetric Analyses.** TGA measurements were performed using a Netzsch STA 449C thermogravimetric analyzer coupled with a Netzsch Aeolos QMS 403C mass spectrometer. A dry solvent-free sample is exposed to 3 drops of solvent, upon which it remains on the benchtop until the excess solvent has evaporated. The dry powder is then loaded into the instrument in which it sits under an air flow until the mass is stabilized. In all experiments, extrusion of the solvent molecules was supported by mass spectrometry. For complexes with acetone binding, experiments were conducted over a range of 150 °C, from 34 to 184 °C. THF experiments were conducted from 35 to 200 °C. Temperature was increased at a rate of 5 °C/min.

**Variable-Temperature NMR Studies.** A known amount of SiMe<sub>4</sub> ( $\delta = 0.00$  ppm) was added in a 5 mL volumetric flask, and the volume was completed with toluene-*d*<sub>8</sub> and then stored at 4 °C between experiments. In all experiments a capillary with 10  $\mu$ L of methanol in 0.1 mL of methanol-*d*<sub>4</sub> was added inside the tube in order to have an internal standard for temperature calibration. Prior to analyses, the chemical shift of acetone in toluene-*d*<sub>8</sub> was measured as a function of temperature. The calibration curve for the chemical shift of acetone from 190 to 330 K gave a linear correlation with the relation  $\delta_{\text{acetone}} = 0.001725T + 1.0436$  ( $R^2 = 0.9966$ ). In the VT-NMR experiments, 5–10 mg of the metallocavitand was dissolved in 0.500 mL of the solution of toluene-*d*<sub>8</sub> containing SiMe<sub>4</sub>. <sup>1</sup>H NMR was taken at room temperature prior to addition of 1 equiv of acetone using a microsyringe. NMR spectra were collected from –90 to 50 °C with 10 °C increments. Thermodynamic values were determined using the following relations, where [Ta·L] is the concentration of the host–guest complex, [L] is the concentration of free acetone, and [acetone] is the overall acetone concentration in the system:

- (1)  $K_{\text{eq}} = [\text{Ta}\cdot\text{L}]/([\text{Ta}]\cdot[\text{L}])$
- (2)  $[\text{acetone}] = [\text{Ta}\cdot\text{L}] + [\text{L}]$
- (3)  $\delta_{\text{observed}} = ([\text{Ta}\cdot\text{L}]\cdot\delta_{\text{Ta}\cdot\text{L}} + [\text{L}]\cdot\delta_{\text{L}})/([\text{Ta}\cdot\text{L}] + [\text{L}])$
- (4) from 3  $[\text{Ta}\cdot\text{L}] = [\text{acetone}](\delta_{\text{L}}\cdot\delta_{\text{observed}})/(\delta_{\text{L}}\delta_{\text{Ta}\cdot\text{L}})$

With knowledge of the  $K_{\text{eq}}$  at various temperatures a Van't Hoff plot was done. Deviation from linearity is observed at lower temperature, which is associated with the lower solubility of the complex, but did not affect significantly the overall trend and the thermodynamic data.

The simulation of the acetone <sup>1</sup>H NMR resonances was done using WINDNMR program. The Va and Vb values were used in order to match those observed experimentally, but the ratio between the included and the free acetone was modified in order to account for the

low solubility of the complex. Typical examples of simulation are shown in the details in the Experimental Section.

**Crystallographic Details.** Crystallographic data were obtained from single crystals coated with Paratone-N oil, mounted using a glass fiber, and frozen in the cold nitrogen stream of the goniometer. All crystals were measured on a Bruker SMART APEX II diffractometer at 200 K with Mo K $\alpha$  radiation except crystals of Ta<sub>3</sub>-Napht and Ta<sub>3</sub>-4PhEt measured at 100 K on a Bruker APEX II diffractometer equipped with an Incoatec Microsource generator producing Cu K $\alpha$  radiation. Data were reduced (SAINT)<sup>17</sup> and corrected for absorption (SADABS).<sup>18</sup> Structure was solved and refined using SHELXS-97 and SHELXL-97.<sup>19</sup> All non-H atoms were refined anisotropically. Hydrogen atoms were placed at idealized positions, but as the hydrogen atoms on the hydroxyl ligands were not found in the difference Fourier map, they were not included in the final model. Crystallographic data are given in Table 5.

## ■ ASSOCIATED CONTENT

### 📄 Supporting Information

Selected NMR spectra, TGA curves, ORTEP of synthesized compounds with included solvents, and thermodynamic and kinetic details. This material is available free of charge via the Internet at <http://pubs.acs.org>. Crystallographic data have been deposited with CCDC (CCDC No. 892323 for Ta<sub>3</sub>-4Ph, CCDC No. 892322 for Ta<sub>3</sub>-4OPh, CCDC No. 892321 for Ta<sub>3</sub>-4OBn, CCDC No. 892320 for Ta<sub>3</sub>-4PhEt, and CCDC No. 892319 for Ta<sub>3</sub>-4Napht). These data can be obtained upon request from the Cambridge Crystallographic Data Centre, 12 Union Road, Cambridge CB2 1EZ, UK, e-mail: [deposit@ccdc.cam.ac.uk](mailto:deposit@ccdc.cam.ac.uk), or via the Internet at [www.ccdc.cam.ac.uk](http://www.ccdc.cam.ac.uk).

## ■ AUTHOR INFORMATION

### ✉ Corresponding Author

\*E-mail: [frederic.fontaine@chm.ulaval.ca](mailto:frederic.fontaine@chm.ulaval.ca).

### Notes

The authors declare no competing financial interest.

## ■ ACKNOWLEDGMENTS

We are grateful to NSERC (Canada), CFI (Canada), FQRNT (Québec), CCVC (Québec), and CERPIC (Université Laval) for financial support. C.N.G. is grateful to NSERC and FQRNT

for scholarships. We acknowledge F. Kleitz and R. Guillet-Nicolas for their help with TGA-MS analyses.

## REFERENCES

- (1) Some leading review articles : (a) Biro, S. M.; Rebek, J., Jr. *Chem. Soc. Rev.* **2007**, *36*, 93–104. (b) Purse, B. W.; Rebek, J., Jr. *Proc. Natl. Acad. Sci.* **2005**, *102*, 10777–10782. (c) Szumna, A. *Chem. Soc. Rev.* **2010**, *39*, 4274–4285. (d) Houk, K. N.; Leach, A. G.; Kim, S. P.; Zhang, X. *Angew. Chem., Int. Ed.* **2003**, *42*, 4872–4897. (e) Marchetti, L.; Levine, M. *ACS Catal.* **2011**, *1*, 1090–1118. (f) Hooley, R. J.; Rebek, J., Jr. *Chem. Biol.* **2009**, *16*, 255–264. Makha, M.; Purich, A.; Colin, L.; Sobolev, A. N. *Eur. J. Inorg. Chem.* **2006**, 507–517.
- (2) Redshaw, C. *Coord. Chem. Rev.* **2003**, *244*, 45–70.
- (3) Yi, J.-M.; Zhang, Y.-Q.; Cong, H.; Xue, S.-F.; Tao, Z. *J. Mol. Struct.* **2009**, *933*, 112–117.
- (4) Jeon, W. S.; Moon, K.; Park, S. H.; Chun, H.; Ko, Y. H.; Lee, J. Y.; Lee, E. S.; Samal, S.; Selvapalam, N.; Rekharsky, M. V.; Sindelar, V.; Sobransingh, D.; Inoue, Y.; Kaifer, A. E.; Kim, K. *J. Am. Chem. Soc.* **2005**, *127*, 12984–12989.
- (5) Few leading references: (a) Shenoy, S. R.; Pinacho Crisóstomo, F. R.; Iwasawa, T.; Rebek, J., Jr. *J. Am. Chem. Soc.* **2008**, *130*, 5658–5659. (b) Zelder, F. H.; Rebek, J., Jr. *Chem. Commun.* **2006**, 753–754. (c) Gissot, A.; Rebek, J., Jr. *J. Am. Chem. Soc.* **2004**, *126*, 7424–7425.
- (6) (a) Kuykendall, D. W.; Zimmerman, S. C. *Nat. Nanotechnol.* **2007**, *2*, 201–202. (b) Memisoglu-Bilensoy, E.; Dogan, A. L.; Hincal, A. A. *J. Pharm. Pharmacol.* **2006**, *58*, 585–589.
- (7) Few leading references: (a) Schramm, M. P.; Rebek, J., Jr. *Chem.—Eur. J.* **2006**, *12*, 5924–5933. (b) Pinalli, R.; Suman, M.; Dalcanale, E. *Eur. J. Org. Chem.* **2004**, 451–462. (c) Arimori, S.; Davidson, M. G.; Fyles, T. M.; Hibbert, T. G.; James, T. D.; Kociok-Köhn, G. I. *Chem. Commun.* **2004**, 1640–1641.
- (8) (a) Jeunesse, C.; Armspach, D.; Matt, D. *Chem. Commun.* **2005**, 5603–5614. (b) Northrop, B. H.; Yang, H.-B.; Stang, P. J. *Chem. Commun.* **2008**, 5896–5980. (c) Frischmann, P. D.; MacLachlan, M. J. *Comments Inorg. Chem.* **2008**, *29*, 26–45. (d) Lenthall, J. T.; Steed, J. W. *Coord. Chem. Rev.* **2007**, *251*, 1747–1760.
- (9) (a) Lejeune, M.; Jeunesse, C.; Matt, D.; Kyritsakas, N.; Welter, R.; Kintzinger, L.-P. *Dalton Trans.* **2002**, 1642–1650. (b) Monnereau, L.; Sémeril, D.; Matt, D.; Toupet, L. *Chem.—Eur. J.* **2010**, *16*, 9237–9247.
- (10) (a) Pluth, M. D.; Bergman, R. G.; Raymond, K. N. *Acc. Chem. Res.* **2009**, *42*, 1650–1659. (b) Yoshizawa, M.; Tamura, M.; Fujita, M. *Science* **2006**, *312*, 251–254. (c) Linton, B.; Hamilton, A. D. *Chem. Rev.* **1997**, *97*, 1669–1680. (d) Frischmann, P. D.; Mehr, H. M.; Patrick, B. O.; Lelj, F.; MacLachlan, M. J. *Inorg. Chem.* **2012**, *51*, 3443–3453.
- (11) (a) Eddaoudi, M.; Moler, D. B.; Li, H.; Chen, B.; Reineke, T. M.; O’Keeffe, M.; Yaghi, O. M. *Acc. Chem. Res.* **2001**, *34*, 319–330. (b) Chun, H.; Jung, H.; Koo, G.; Jeong, H.; Kim, D.-K. *Inorg. Chem.* **2008**, *47*, 5355–5359. (c) Sato, T.; Mori, W.; Kato, C. N.; Yanaoka, E.; Kuribayashi, T.; Ohtera, R.; Shiraishi, Y. *J. Catal.* **2005**, *232*, 186–198.
- (12) (a) Ahijado, M.; Braun, T. *Angew. Chem., Int. Ed.* **2008**, *47*, 2954–2958. (b) Zhao, P.; Incarvito, C. D.; Hartwig, J. F. *J. Am. Chem. Soc.* **2007**, *129*, 1876–1877. (c) Crociani, B.; Antonaroli, S.; Marini, A.; Matteoli, U.; Scrivanti, A. *Dalton Trans.* **2006**, 2698–2705. (d) Pantcheva, I.; Osakada, K. *Organometallics* **2006**, *25*, 1735–1741. (e) Pantcheva, I.; Nishihara, Y.; Osakada, K. *Organometallics* **2005**, *24*, 3815–3817. (f) Balkwill, J. E.; Cole, S. C.; Coles, M. P.; Hitchcock, P. B. *Inorg. Chem.* **2002**, *41*, 3548–3552. (g) Marlin, D. S.; Bill, E.; Weyhermüller, T.; Bothe, E.; Wieghardt, K. *J. Am. Chem. Soc.* **2005**, *127*, 6095–6108. (h) Duboc-Toia, C.; Hummel, H.; Bill, E.; Barra, A.-L.; Chouteau, G.; Wieghardt, K. *Angew. Chem., Int. Ed.* **2000**, *39*, 2888–2890. (i) Bossek, U.; Hummel, H.; Weyhermüller, T.; Wieghardt, K.; Russell, S.; van der Wolf, L.; Kolb, U. *Angew. Chem., Int. Ed.* **1996**, *35*, 1552–1554. (j) Bardwell, D. A.; Jeffery, J. C.; Ward, M. D. *Polyhedron* **1996**, *15*, 2019–2022.
- (13) (a) Sigouin, O.; Garon, C. N.; Delaunais, G.; Yin, X.; Woo, T. K.; Decken, A.; Fontaine, F.-G. *Angew. Chem., Int. Ed.* **2007**, *46*, 4979–
4982. (b) Garon, C. N.; Goreslky, S. I.; Sigouin, O.; Woo, T. K.; Fontaine, F.-G. *Inorg. Chem.* **2009**, *48*, 1699–1710.
- (14) Ooi, T.; Kondo, Y.; Maruoka, K. *Angew. Chem., Int. Ed.* **1998**, *37*, 3039–3041.
- (15) Turi, L. *Chem. Phys. Lett.* **1997**, *275*, 35–39.
- (16) Sanner, R. D.; Carter, S. T., Jr. *J. Organomet. Chem.* **1982**, *240*, 157–162.
- (17) Bruker. SAINT, Version 7.07a; Bruker AXS Inc.: Madison, WI, 2003.
- (18) Sheldrick, G. M. SADABS, Version 2004/1; Bruker AXS Inc.: Madison, WI, 2004.
- (19) Sheldrick, G. M. *Acta Crystallogr.* **2008**, *A64*, 112–122.